Applied Catalysis A: General 406 (2011) 102–112

Contents lists available at ScienceDirect

Applied Catalysis A: General

journal homepage: www.elsevier.com/locate/apcata

IR study of active sites for *n*-heptane isomerization over MoO_3-ZrO_2

Nurun Najwa Ruslan[a], Nurrulhidayah Ahmad Fadzlillah[a], Ainul Hakimah Karim[a], Aishah Abdul Jalil[b], Sugeng Triwahyono[a,*]

[a] Ibnu Sina Institute for Fundamental Science Studies, Faculty of Science, Universiti Teknologi Malaysia, 81310 UTM Johor Bahru, Johor, Malaysia
[b] Department of Chemical Engineering, Faculty of Chemical Engineering, Universiti Teknologi Malaysia, 81310 UTM Johor Bahru, Johor, Malaysia

ARTICLE INFO

Article history:
Received 25 May 2011
Received in revised form 10 August 2011
Accepted 12 August 2011
Available online 22 August 2011

Keywords:
MoO_3-ZrO_2
Lewis acid sites
Protonic (Brönsted) acid sites
Monoclinic ZrO_2
Tetragonal ZrO_2

ABSTRACT

The property of acidic sites on MoO_3-ZrO_2 was studied for *n*-heptane isomerization. A 2,6-lutidine IR study showed that the introduction of MoO_3 on ZrO_2 partially eliminated the absorbance band at 1605 cm^{-1} ascribed to Lewis acid sites corresponding to the presence of the monoclinic phase of ZrO_2 and developed several Brönsted and Lewis acid sites with different acidic strengths. MoO_3-ZrO_2 possesses a large number of relatively weak Lewis and Brönsted acid sites as well as strong acid sites. The active protonic acid sites in *n*-heptane isomerization were formed from molecular hydrogen through a spillover mechanism with the involvement of doublet bands at 1595 and 1580 cm^{-1} ascribed to the Lewis acid sites corresponding to the presence of the tetragonal phase of ZrO_2. No catalytic activity of MoO_3-ZrO_2 for *n*-heptane isomerization was observed in the absence of the doublet bands at 1595 and 1580 cm^{-1} and hydrogen in the gas phase.

1. Introduction

Molybdenum oxide catalysts supported on SiO_2, Al_2O_3, ZrO_2 and TiO_2 have been extensively studied in recent years due to their possible ability to catalyze the isomerization of linear alkanes [1–4]. The isomerization of linear alkanes is a key process for the production of high-quality liquid fuels. Therefore, many researchers are currently exploring the preparation, characterization and utilization of catalysts for the isomerization process. Among them, MoO_3-ZrO_2 has attracted attention due to the properties of the ZrO_2 support, which is able to provide strong acidic sites when mixed with another metal oxide or acidic ion such as WO_3 or SO_4^{2-} [5,6]. It is well known that the preparation methods can produce a zirconia-based catalyst with different chemical, physical and catalytic properties. Calafat et al. [7] and Bhaskar et al. [5] reported that the incorporation of molybdenum with zirconia through coprecipitation yields mixed oxides that have a higher surface area and are more easily reduced, leading to higher catalytic activity. Adamski et al. prepared a series of MoO_3-ZrO_2 catalysts by slurry deposition and reported that the presence of MoO_3 has no influence on the phase composition of ZrO_2 support [8]. On the other hand, Afanasiev investigated the effect of the sintering process on different prepared MoO_3-ZrO_2 catalysts [9]. He reported that the monolayer dispersion can be obtained either from the sintering of high surface-area dispersion or from the heating process during preparation of the catalyst. Conversely, Samaranch et al. investigated the effect of MoO_3 loading on the structure, acidic and catalytic properties of MoO_3-ZrO_2 by sol–gel method [10]. As the MoO_3 loading increased, the surface area of the catalyst increased with simultaneous formation of Brönsted acid sites due to the presence of surface polymolybdate species [10]. Meanwhile, the catalyst prepared by wet impregnation method has also been widely studied [11,12]. In this case, the nuclearity of molybdenum species is mostly controlled by the acid–base properties of support sites.

Among many different catalytic applications of MoO_3-ZrO_2, alkane isomerization [13], methane and 2-butene oxidation [14,15], isobutene/butane alkylation [16], methylcyclopentane conversion [17], 3-picoline ammoxidation [5] and dehydration of 2-propanol [10,18] can be focused on due to the nature of specific interactions between MoO_3 with ZrO_2 that influenced the molecular structure of the surface oxomolybdenum species, which essential for catalyst selectivity. The majority of the reactions require strong acidic sites in order to occur. The incorporation of MoO_3 on ZrO_2 increases the acidic character of ZrO_2 and some studies have even demonstrated the appearance of superacidity when modified with SO_4^{2-} and WO_3 [19,20].

Although research has been published on the MoO_3-ZrO_2 catalyst, an understanding of its properties to improve the activity and stability of this catalyst is lacking. In previous studies, an increase in the catalytic activity of MoO_3-ZrO_2 has been proposed based on the changes in crystallinity, surface area and acidity of MoO_3-ZrO_2 [8–10]. However, no report or evidence related to the active sites for

* Corresponding author. Tel.: +60 75536076; fax: +60 75536080.
E-mail address: sugeng@ibnusina.utm.my (S. Triwahyono).

0926-860X/$ – see front matter © 2011 Elsevier B.V. All rights reserved.
doi:10.1016/j.apcata.2011.08.014

acid catalytic reaction over MoO_3-ZrO_2 has been published to date. In this study, we report the results of an IR study and *n*-heptane isomerization on MoO_3-ZrO_2. The adsorption of pyridine and 2,6-lutidine base probe molecules were monitored by IR spectroscopy and used to confirm type, strength and the evolution of acid sites in contact with hydrogen in gas phase. Pyridine is a common probe molecule to distinguish Lewis and Brönsted acid sites whereas the use of 2,6-lutidine allows confirming the strength of Brönsted acid sites due to the sterically hindered amine on Lewis acid sites. In general, substituted amine may not undergo such interaction with Lewis acid sites due to the steric effect. However, in the presence of strong Lewis acid sites, this type of amine has been a specific probe molecule to identify Brönsted acid sites. In this study, we have successfully demonstrated the formation of protonic acid sites through the H-spillover phenomenon over MoO_3-ZrO_2 evidenced by 2,6-lutidine preadsorbed IR study in which 2,6-lutidine probe molecules exclusively reveal the participation of tetragonal phase zirconia in the formation of protonic acid sites. The high activity and stability of MoO_3-ZrO_2 for *n*-heptane isomerization was strongly determined by the presence of active protonic acid sites from spillover hydrogen.

2. Experimental

2.1. Catalyst preparation

MoO_3-ZrO_2 was prepared as follows. Zirconium hydroxide ($Zr(OH)_4$) was prepared from an aqueous solution of $ZrOCl_2{\cdot}8H_2O$ (Wako Pure Chemical) by hydrolysis with 2.8 wt% NH_4OH aqueous solution [21]. The final pH value of the supernatant was 9.0. The precipitate was filtered and washed with deionized water. The gel obtained was dried at 383 K to form $Zr(OH)_4$. Ammonium heptamolybdate ($(NH_4)_6Mo_7O_{24}{\cdot}4H_2O$) was prepared by the addition of MoO_3 [22] with 2.8 wt% NH_4OH aqueous solution at 353 K. The MoO_3-ZrO_2 catalyst was prepared by impregnation of $Zr(OH)_4$ with ammonium heptamolybdate solution at 353 K under vigorous stirring conditions. The resulting material was dried overnight at 383 K followed by calcination at 1093 K for 3 h. The surface of MoO_3-ZrO_2 area was 56 m^2/g and the content of Mo was 5 wt%.

2.2. Characterization of catalyst

The crystalline structure of catalysts was determined with X-ray diffraction (XRD) recorded on a Bruker AXS D8 Automatic Powder Diffractometer using Cu Kα radiation with λ = 1.5418 Å at 40 kV and 40 mA over a range of $2\theta = 20$–40°. The fraction of the tetragonal phase of ZrO_2 in the sample was determined based on the formula proposed by Toraya and Yoshimura [23].

$$V_t = 1 - \frac{1.31X_m}{1 + 0.31X_m} \quad (1)$$

$$X_m = \frac{I_m(11\bar{1}) + I_m(1\,1\,1)}{I_m(11\bar{1}) + I_m(1\,1\,1) + (1\,1\,1)} \quad (2)$$

where X_m is the intensity ratio of monoclinic ZrO_2. $I_t(1\,1\,1)$, $I_m(1\,1\,1)$ and $I_m(11\bar{1})$ are the integrated intensity of the (1 1 1) reflection of the tetragonal phase at $2\theta = 30.2^\circ$, (1 1 1) reflection of the monoclinic phase at $2\theta = 31.8^\circ$ and $(11\bar{1})$ reflection of the monoclinic phase of ZrO_2 at $2\theta = 28.2^\circ$, respectively, while 1.31 is Toraya's theoretical deviation from the linearity value.

The surface density of MoO_3, ρ_{MnO_3} is determined by the following equation:

$$\rho_{MnO_3}\left[\frac{MoO_3\ \text{atoms}}{nm^2\ \text{samples}}\right] = \frac{\frac{\text{wt\% MoO}_3}{100}\left[\frac{\text{g MoO}_3}{\text{g sample}}\right] \times \frac{1}{\text{MW MoO}_3}\left[\frac{\text{mol MoO}_3}{\text{g MoO}_3}\right] \times \text{NA}\left[\frac{\text{MoO}_3\ \text{atoms}}{\text{mol MoO}_3}\right]}{\text{SA sample}\left[\frac{\text{nm}^2\ \text{sample}}{\text{g sample}}\right]} \quad (3)$$

where MW_{MnO_3}, NA and SA are the molecular weight of MoO_3, Avogadro number and the specific surface area of the sample, respectively.

The specific surface area of the catalysts was determined with a Quantachrome Autosorb-1 at 77 K. Prior to the analysis, the sample was outgassed at 573 K for 3 h. Surface morphology and elemental composition analysis were performed using a Field Emission Scanning Electron Microscopy-Energy Dispersive X-Ray (JEOL JSM-6701F) with an accelerating voltage of 15 kV.

In the measurement of IR spectra, a self-supported wafer placed in an in situ stainless steel IR cell with CaF_2 windows was activated with a hydrogen flow at 623 K for 3 h, followed by outgassing at 623 K for 2 h [24]. For 2,6-lutidine adsorption, 2 Torr of 2,6-lutidine was adsorbed on activated samples at room temperature for 30 min followed by outgassing at 473 K. The effect of the activation temperature of the sample was observed at 473, 573 and 623 K, while the effect of 2,6-lutidine outgassing was observed at room temperature, 373 and 473 K. For pyridine adsorption, 2 Torr of pyridine was adsorbed on activated samples at 423 K for 30 min followed by outgassing at 573 K for 30 min. To observe the strength and distribution of acidic sites, pyridine adsorption was studied on the sample activated at 573, 598 and 623 K and pyridine outgassing at different temperatures of 423, 473, 523 and 573 K. The formation of protonic acid sites from molecular hydrogen was observed as follows [25,26]. A 2,6-lutidine or pyridine pre-adsorbed sample was exposed to 25 Torr of hydrogen at room temperature. The sample was then heated stepwise to 473 K in 50 K increments. Because the sample had been activated with hydrogen at 623 K, the sample was not reduced further on contact with hydrogen at a temperature of 473 K and below. The removal of protonic acid sites was done at room temperature to 523 K. All spectra were recorded on a Perkin-Elmer Spectrum GX FT-IR Spectrometer at room temperature.

2.3. Hydrogen adsorption

The hydrogen uptake was measured using the automatic gas adsorption apparatus Belsorp-28SA. A catalyst sample was placed in an adsorption vessel and activated in a hydrogen flow at 623 K for 3 h followed by evacuation at 623 K for 3 h. The sample was subsequently cooled to an adsorption temperature of 473 K and held for 3 h in order to stabilize the temperature [27,28]. Twenty five Torr of hydrogen was then introduced into the adsorption system and the pressure change was monitored to calculate the hydrogen uptake.

2.4. Isomerization of n-heptane

The isomerization of *n*-heptane was conducted at 573 K in a microcatalytic pulse reactor equipped with an online sampling valve for gas chromatographic analysis [29]. A 0.4-g portion of the sample was charged into an ID10 mm tubular reactor and then was subjected to H_2 reduction at 623 K for 12 h ($F_{Hydrogen}$ = 100 mL/min). Isomerization was conducted at 573 K in the presence of hydrogen or nitrogen carrier gas. The products were analyzed by an online 6090N Agilent Gas Chromatograph equipped with FID and VZ7 packed columns.

The selectivity to a particular product (S_i) was calculated according to Eq. (4).

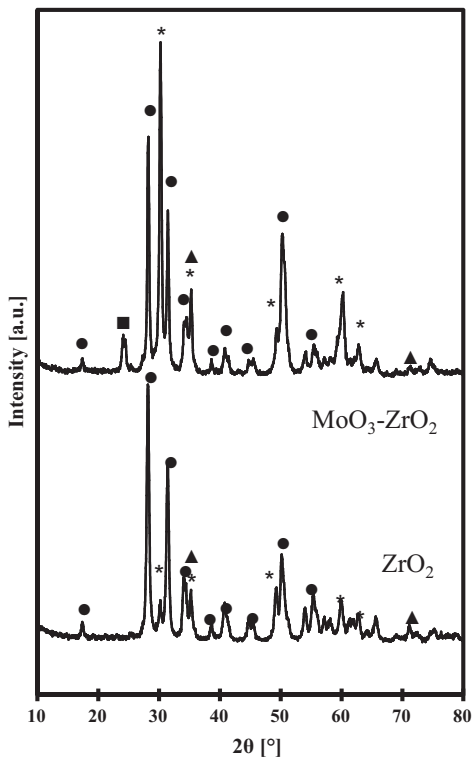

Fig. 1. X-ray diffraction patterns of ZrO_2 and MoO_3-ZrO_2. (●) Monoclinic phase of ZrO_2; (*) tetragonal phase of ZrO_2; (▲) cubic phase of ZrO_2; (■) $Zr(MoO_4)_2$ phase.

$$S_i = \frac{A_i}{\sum A_i - A_{n\text{-heptane}}} \times 100 \quad (4)$$

where A_i is the corrected chromatographic area for a particular compound. The conversion of reactant (X) was determined by Eq. (5).

$$X_{n\text{-heptane}} = \frac{\sum A_i - A_{n\text{-heptane}}}{\sum A_i} \quad (5)$$

3. Results and discussion

3.1. Crystalline structure of the catalyst

Fig. 1 shows the XRD pattern of ZrO_2 and MoO_3-ZrO_2 calcined at 1093 K. ZrO_2 exhibited three well-established polymorphs: the monoclinic, tetragonal and cubic phase of ZrO_2. The sharp diffraction lines at $2\theta = 17.3°$, 28.2°, 31.5°, 33.9°, 38.4°, 40.6°, 44.5°, 50.1° and 55.3° correspond to the monoclinic phase of ZrO_2, peaks at $2\theta = 30.2°$, 34.3°, 49.1°, 59.7° and 62.6° correspond to the tetragonal phase of ZrO_2, while the peaks at $2\theta = 32.9°$ and 70.4° correspond to cubic phase of ZrO_2. The introduction of MoO_3 on ZrO_2 partially eliminated the peaks ascribed to the monoclinic phase of ZrO_2 and developed new peaks ascribed to the tetragonal phase of ZrO_2. In addition, a new small peak was observed at $2\theta = 23.9°$ which may be related to the presence of $Zr(MoO_4)_2$ hexagonal phase [30]. The presence of MoO_3 delayed or inhibited the sintering of ZrO_2 crystallites, which led to the stabilization of the tetragonal phase of ZrO_2. The fraction of the tetragonal phase of ZrO_2 increased from 0.17 to 0.51 by the addition of MoO_3. Samaranch et al. reported a progressive stabilization effect of the tetragonal phase of ZrO_2 with an increase in MoO_3 loading [10]. The presence of monoclinic and tetragonal phases of ZrO_2 was observed for 1–6% MoO_3 content and the further loading of MoO_3 diminished the monoclinic phase of ZrO_2. The stabilization effect of the tetragonal phase of ZrO_2 was also observed on WO_3- and SO_4^{2-}-loaded ZrO_2. Scheithauer et al. reported that the monoclinic phase of ZrO_2 dominated at 7.5 wt% WO_3 and was lower when the sample was calcined at 1098 K [31]. An increase in WO_3 loading up to 19 wt% WO_3 increased the fraction of the tetragonal phase of ZrO_2. This result indicates that minimum WO_3 loading is required to inhibit the formation of the monoclinic phase of ZrO_2. Our research group has previously reported on the effect of sulfate ion loading on the stabilization effect of the tetragonal phase of ZrO_2 [21]. The tetragonal phase is the dominant structure of ZrO_2 for 1.0 N sulfate ion loading and below. The excess sulfate ion amount collapsed the tetragonal phase of ZrO_2, and new peaks associated with the monoclinic phase of ZrO_2 developed on 4.0 N of sulfate ion content.

The specific surface area of ZrO_2 obtained by calcination of zirconium hydroxide at 1029 K was 42 m^2/g and the introduction of MoO_3 increased the specific surface area to 56 m^2/g. The increase may be related to the elimination of the monoclinic phase of ZrO_2 and the development of new tetragonal phases of ZrO_2. The change in the specific surface area caused by the introduction of MoO_3 on ZrO_2 has been reported by several research groups. Afanasiev [9] and Yori et al. [13] concluded that the specific surface area of binary MoO_3-ZrO_2 was not significantly affected by the calcination temperature during preparation but is more determined by the number of tetragonal phases of ZrO_2 in the sample. The transformation of the tetragonal to monoclinic phase of ZrO_2 reduced the specific surface area of the sample markedly. Meanwhile, Samaranch et al. reported that the sol–gel method provided a high surface area of MoO_3-ZrO_2, and the maximum surface area was observed for 15–17 wt% MoO_3 loading of ZrO_2 [10].

Fig. 2 shows the FE-SEM image and EDX analysis of MoO_3-ZrO_2. FE-SEM images showed irregular shapes and aggregations of the MoO_3-ZrO_2 sample, with the aggregation size approximately 100 nm. EDX analysis results showed that the average wt% ratio of Mo/Zr was approximately 0.09, which is equivalent to 3.7 MoO_3/nm^2-cat.

3.2. Acidity of MoO_3-ZrO_2

2,6-Lutidine ($pK_b = 7.4$), which has a more basic property than pyridine ($pK_b = 8.8$), is used to evaluate the acidity of catalysts, particularly in the observation of the relatively weak Brönsted acid sites and the acidic centers of Lewis acid site types [32,33]. Fig. 3 shows the spectra of 2,6-lutidine adsorbed on ZrO_2 and MoO_3-ZrO_2 activated at different temperatures and different outgassing of 2,6-lutidine. Two characteristic absorbance bands arose below and above 1620 cm^{-1}, which are ascribed to the 2,6-lutidine species adsorbed on Lewis and Brönsted acid sites, respectively. The introduction of MoO_3 partially eliminated the absorbance band at 1605 cm^{-1} and developed new absorbance bands at 1595 cm^{-1} (broad and asymmetric) and 1590 cm^{-1} (sharp and symmetric) corresponding to the Lewis acid sites related to tetragonal and monoclinic phases of ZrO_2, respectively [33]. Other absorbance bands appeared at 1660, 1640 and 1630 cm^{-1} corresponding to the Brönsted acid sites. The decrease in the absorbance band at 1605 cm^{-1} might be related to the interaction of MoO_3 with Lewis acid sites corresponding to the monoclinic phase of ZrO_2 through O, resulting in the development of new Lewis and Brönsted acid sites with different acidic strengths and acidic centers. The remaining shoulder peak at 1605 cm^{-1} might indicate the presence of the monoclinic phase of ZrO_2, which did not interact with MoO_3. Intensification of the absorbance band at 1580 cm^{-1} reflected the superposition of the absorbance bands attributed to 2,6-lutidine species adsorbed in molecular form and H-bonded 2,6-lutidine on both Lewis acid sites corresponding to the tetragonal and monoclinic phases of ZrO_2.

On the basis of literature data on 2,6-lutidine adsorption [33–35], the adsorption on MoO_3-ZrO_2 in this experiment can be summarized as follows:

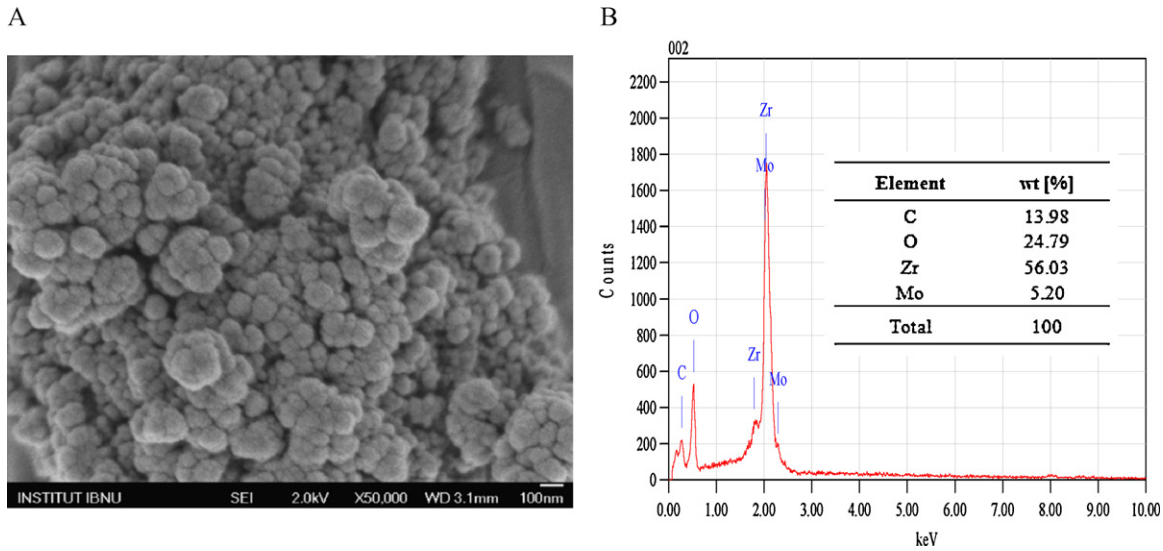

Fig. 2. (A) FE-SEM image of MoO_3-ZrO_2, (B) EDX spectra of MoO_3-ZrO_2.

i) In the ZrO_2 sample, the doublet bands ascribed to physisorbed and/or H-bonded 2,6-lutidine on Lewis acid sites were observed at 1605 (8a mode) and 1580 (8b mode) cm^{-1} (Fig. 3A inset). These bands corresponded to the presence of the monoclinic phase of ZrO_2, whereas no significant band ascribed to Brönsted acid sites was observed on the ZrO_2 sample.

ii) For the Lewis acid sites on the MoO_3-ZrO_2 sample, physisorbed and/or H-bonded 2,6-lutidine on Lewis acid sites corresponding to the monoclinic phase of zirconia were observed as dual doublets; one set was at 1605 (8a mode) and 1580 (8b mode) cm^{-1} as well as ZrO_2, and the other set was at 1590 (8a mode) and 1580 (8b mode) cm^{-1}. However, the doublet bands of Lewis acid sites related to the tetragonal phase of ZrO_2 were observed at 1595 (8a mode) and 1580 (8b mode) cm^{-1}.

iii) For the Brönsted acid sites on the MoO_3-ZrO_2 sample, strong doublet bands at 1640 and 1630 cm^{-1} were observed due to the 8a and 8b mode of protonated 2,6-lutidine species adsorbed on Brönsted acid sites. In addition, a shoulder band at 1660 cm^{-1} was due to the 8a mode of protonated 2,6-lutidine species adsorbed on Brönsted acid sites. As a partner of the 1660 cm^{-1} band, a shoulder band at 1645 cm^{-1} (8b mode) was observed after outgassing at 373 K and above.

Samaranch et al. reported the adsorption of lutidine on MoO_3-ZrO_2 for the detection of Lewis and protonic acid sites [10]. For low

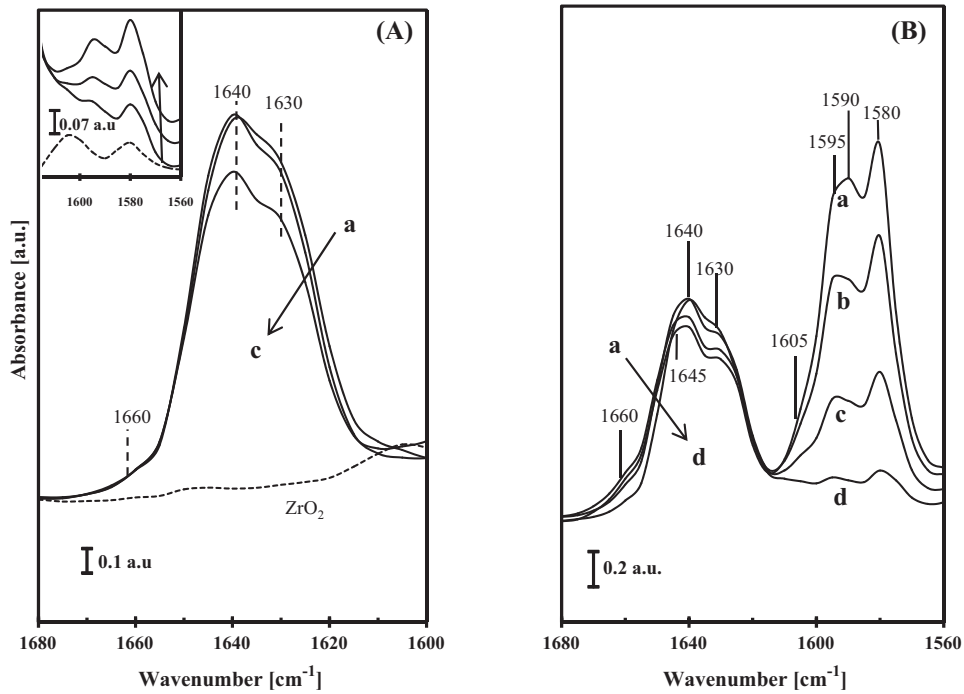

Fig. 3. (A) IR spectra of Brönsted and Lewis acid sites region when 2,6-lutidine was adsorbed on MoO_3-ZrO_2 samples activated at different temperatures. Samples were activated at (a) 473 K, (b) 573 K and (c) 598 K. Inset shows spectra of Lewis acid sites region. Dotted lines represent the 2,6-lutidine adsorbed on ZrO_2. (B) IR spectra of 2,6-lutidine adsorbed on MoO_3-ZrO_2 samples activated at 598 K (dotted lines), followed by 2,6-lutidine adsorption at (a) room temperature and outgasssed at (b) room temperature, (c) 373 K and (d) 473 K.

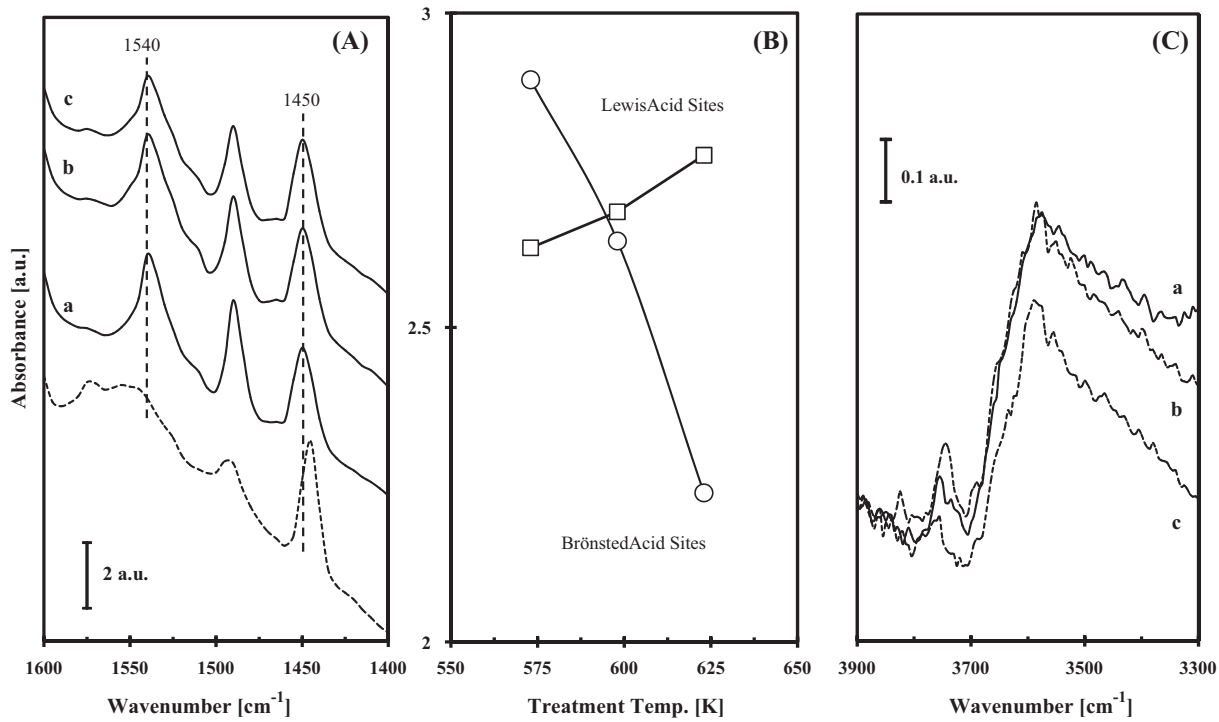

Fig. 4. (A) IR spectra of pyridine adsorbed on MoO_3-ZrO_2 samples activated at different temperatures. Samples were activated at (a) 573 K, (b) 598 K, and (c) 623 K. Pyridine was adsorbed at 423 K and outgassed at 573 K. Dotted lines represent pyridine adsorbed on ZrO_2. (B) Variations of the absorbance of the IR bands for Brönsted and Lewis acid sites with the treatment temperature of sample. (C) The change of the absorbance of the IR bands for OH region of samples activated at (a) 573 K, (b) 598 K, and (c) 623 K.

MoO_3 content, the band ascribed to the presence of Lewis and protonic acid sites was observed at 1581, 1612, 1640 and 1630 cm^{-1}. For higher MoO_3 content, the band was observed at 1615 and 1630 cm^{-1} for Lewis and protonic acid sites, respectively. In addition, they also reported that the increase in the MoO_3 content up to 23 wt% increased the number of protonic acid sites and the further increase of MoO_3 decreased the protonic acid sites gradually due to the presence of multilayer MoO_3 on the surface sample. A detailed IR study on the effects of calcination and crystallinity of zirconia for 2,6-lutidine adsorption on sulfated zirconia was reported by Morterra et al. [33]. Thus, on the basis of the frequency number of 2,6-lutidine on the samples, we concluded that the amount of MoO_3 loaded on ZrO_2 in this experiment was low and less than one layer of MoO_3 on ZrO_2. This result is consistent with the presence of the residual band at 1605 cm^{-1} and low MoO_3 content on ZrO_2 indicated the presence of ZrO_2 that did not interact with MoO_3.

Fig. 3A shows the IR spectra of 2,6-lutidine adsorbed on ZrO_2 and MoO_3-ZrO_2 samples activated at different temperatures. The 2,6-lutidine was adsorbed at room temperature for 30 min followed by outgassing at 473 K for 30 min. Therefore, 2,6-lutidine adsorbed on Lewis and Brönsted acid sites under this condition was that which was retained against an outgassing temperature of 473 K and below. As the activation temperature of MoO_3-ZrO_2 increased, the absorbance bands attributed to Brönsted acid sites (bands at 1640 and 1630 cm^{-1}) decreased with a simultaneous increase in the absorbance bands attributed to Lewis acid sites (bands at 1595 and 1580 cm^{-1}) due to the dehydration and/or dehydroxylation process, while there was no change in the shoulder band at 1660 cm^{-1}. This result is similar to other mixed metal oxides such as silica-alumina [36], WO_3-ZrO_2 [25] and zeolitic materials [37] activated at high-temperature eliminated OH groups, leaving Lewis acid sites. Fig. 3B shows the acid strength distribution on activated MoO_3-ZrO_2. 2,6-lutidine was adsorbed at room temperature for 30 min, followed by outgassing at room temperature, 373 and 473 K. The outgassing of adsorbed 2,6-lutidine at 573 K and above diminished the absorbance bands at Lewis acid sites. All absorbance bands ascribed to 2,6-lutidine adsorbed on Lewis and Brönsted acid sites decreased with the outgassing temperature. Although the decrease in Lewis acid sites was higher than that of Brönsted acid sites due to the strong and complex interaction between protonated 2,6-lutidine and Brönsted acid sites [33], the strength distributions of both Lewis and Brönsted acid sites persisted. Based on a 2,6-lutidine probe molecule, the strength distribution might be wider for Lewis acid sites compared to that of Brönsted acid sites. It should be noted that the absorbance band at 1590 cm^{-1} due to the 8a mode of 2,6-lutidine disappeared in the outgassing at 473 K. This band might correspond to the physisorbed 2,6-lutidine and/or H-bounded 2,6-lutidine interaction with weak Lewis acid sites related to the presence of the monoclinic phase of ZrO_2. Indeed, this band was also not observed on the ZrO_2 sample in which the pre-adsorbed 2,6-lutidine was outgassed at 473 K, as shown in Fig. 3A (inset).

The use of a pyridine basic probe molecule for evaluation of the acidity of solid material is essentially the same as that of 2,6-lutidine. Pyridine is more suitable for use in the quantitative evaluation of Brönsted and Lewis acid sites regardless of the acidic centers. Fig. 4 shows the IR spectra of pyridine adsorbed on ZrO_2 and MoO_3-ZrO_2 samples activated at different temperatures. The pyridine was adsorbed at 423 K for 30 min and outgassed at 573 K for 30 min. The ZrO_2 sample possessed Lewis acid sites at 1447 cm^{-1} due to the presence of cus Zr^{4+}, while the broad band in the range of 1525–1575 cm^{-1} may be an artifact produced during preparation of the sample. In fact, the 2,6-lutidine adsorption confirmed the dearth of Brönsted acid sites at >1620 cm^{-1} on the unmodified ZrO_2 sample. The modification of this ZrO_2 with MoO_3 induced strong Brönsted acid sites at 1540 cm^{-1} and Lewis acid sites at 1450 cm^{-1}. The band ascribed to the Lewis acid site at 1447 cm^{-1} on ZrO_2 shifted to a higher frequency at 1450 cm^{-1}; the shift must be due to the interaction of MoO_3 with cus Zr^{4+} through O.

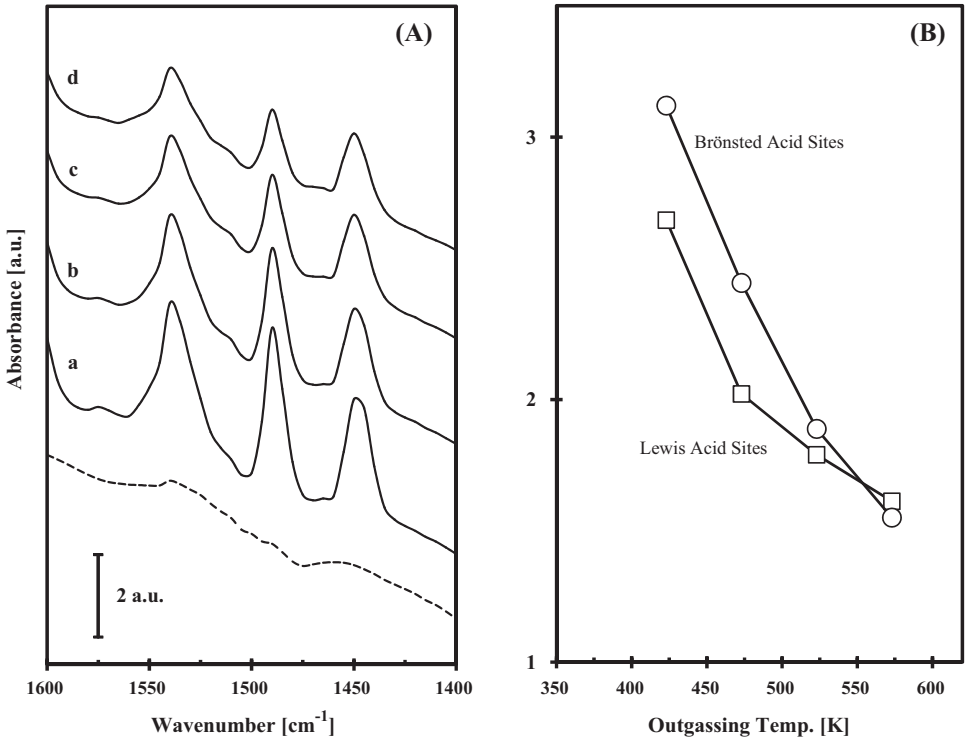

Fig. 5. (A) IR spectra of pyridine adsorbed on MoO_3-ZrO_2 samples activated at 598 K (dotted lines), followed by pyridine adsorption at 423 K and outgasssed at (a) 423 K, (b) 473 K, (c) 523 K, and (d) 573 K. (B) Variations of the absorbance of the IR bands for Brönsted and Lewis acid sites as a function of outgassing temperature after pyridine adsorption for MoO_3-ZrO_2.

High intensities of both acidic sites were observed for MoO_3-ZrO_2 samples activated at 573, 598 and 623 K (Fig. 4A). As the activation temperature of MoO_3-ZrO_2 increased, the absorbance band at 1540 cm^{-1} decreased markedly, while the absorbance band at 1450 cm^{-1} increased considerably with temperature. The changes are clearly seen if the intensities of the absorbance bands at 1540 and 1450 cm^{-1} are plotted against the activation temperature of the sample (Fig. 4B). The ratio of Lewis to Brönsted acid sites increased markedly with increasing activation temperature. Fig. 4C shows the decrease of broad bands ascribed to the OH groups in the range of 3400–3800 cm^{-1} caused by increasing the activation temperature of MoO_3-ZrO_2. Although the locations of surface OH groups on MoO_3-ZrO_2 are not certain at present, the decrease in OH group regions with temperature suggests that the Lewis acid sites are formed by elimination of the surface OH groups at the same locations as protonic acid sites.

Fig. 5 shows the acid strength distribution for activated MoO_3-ZrO_2 when pyridine was used as a probe molecule. The pyridine was adsorbed at 423 K for 30 min and outgassed at 423, 473, 523 and 573 K for 30 min, respectively. Compared to that of the 2,6-lutidine probe molecule, pyridine adsorbed on both Lewis and Brönsted acid sites decreased significantly with outgassing temperature and the decrease still continued up to a temperature of 598 K (Fig. 5B). This result confirmed that the acid strength distribution is similar for both Lewis and Brönsted acid sites on MoO_3-ZrO_2 regardless of the acidic center; a large number of relatively weak Lewis and Brönsted acid sites as well as strong Lewis and Brönsted acid sites exist at 598 K and below. The acid sites distributions observed for MoO_3-ZrO_2 are different from our previous report on WO_3-ZrO_2 [25]. For WO_3-ZrO_2, the acid strength distribution was wide for Lewis acid sites and limited for protonic acid sites. Weak and strong Lewis acid sites and only strong protonic acid sites existed on the WO_3-ZrO_2 sample. It is not certain at present the cause of the difference in the distribution of protonic acid sites between WO_3-ZrO_2 and MoO_3-ZrO_2 in this experiment. The surface density of WO_3 and MoO_3 was 5.6 and 3.7 nm^{-2}-cat, respectively, for which these values correspond to about one monolayer for WO_3 [38] and less than one monolayer for MoO_3 [39] on the surface of ZrO_2. The existence of ZrO_2 on the surface was noticeable, as was MoO_3 for MoO_3-ZrO_2. In reality, the presence of the peak at 1605 cm^{-1} ascribed to 2,6-lutidine adsorption on Lewis acid sites elucidated the presence of cus Zr^{4+}, which does not interact with MoO_3 species. However, in theory 5.6 WO_3/nm^2-cat entirely covered the surface of ZrO_2 [25]. As a result, it is plausible that the presence of both MoO_3 and ZrO_2 on the surface sample caused a wider acid strength distribution of the MoO_3-ZrO_2 sample.

3.3. Protonic acid sites induced by molecular hydrogen

The formation of protonic acid sites from molecular hydrogen through a spillover mechanism on the surface of MoO_3-ZrO_2 was observed by heating 2,6-lutidine pre-adsorbed MoO_3-ZrO_2 in hydrogen gas. Fig. 6A and B show the changes of the IR spectra within a range of 1680–1560 cm^{-1}. Heating of MoO_3-ZrO_2 in hydrogen gas increased the doublet absorbance bands of protonic acid sites at 1640 and 1630 cm^{-1} as long as the decreased in Lewis acid sites simultaneously corresponded to the tetragonal phase of ZrO_2 at 1595 and 1580 cm^{-1}, while the Lewis acid sites corresponding to the monoclinic phase of ZrO_2 at 1605 and 1590 cm^{-1} were not observed after outgassing at 473 K. This suggests that only the Lewis acid sites corresponding to the tetragonal phase of ZrO_2 are involved in the formation of protonic acid sites. It should be noted that the changes in the intensity of absorbance bands ascribed to Lewis and protonic acid sites are not comparable due to the different extinction coefficients for both Lewis and Brönsted acid sites and the complexity of the adsorption of 2,6-lutidine on both acidic sites, particularly on Brönsted acid sites. The change of protonic acid sites on hydroxyl group stretching regions at 1600–1680 cm^{-1} from

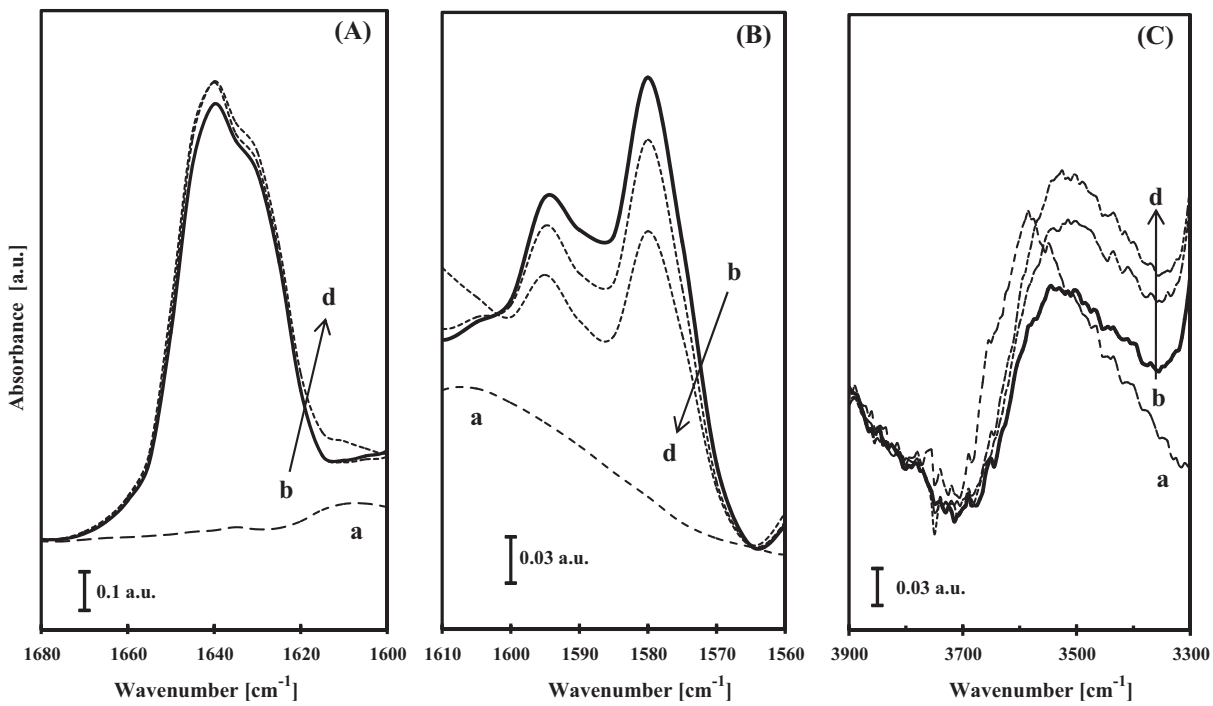

Fig. 6. IR spectra of 2,6-lutidine adsorbed on (a) activated MoO_3-ZrO_2. Spectral changes of (A) protonic acid site, (B) Lewis acid sites and (C) OH groups regions when 2,6-lutidine-preadsorbed sample was heated in hydrogen at (c) 323 K and (d) 473 K. (b) Before exposure to hydrogen.

molecular hydrogen is consistent with the same behavior of the OH stretching region at 3400–3800 cm^{-1} of H-bonded hydroxyl groups when 2,6-lutidine pre-adsorbed with MoO_3-ZrO_2 was heated in the presence of hydrogen gas (Fig. 6C). The broad band ascribed to hydroxyl groups at 3400–3800 cm^{-1} weakened and shifted to a lower frequency with the introduction of 2,6-lutidine. With heating in the presence of hydrogen, the broad band at 3400–3800 cm^{-1} grew continuously with increasing temperature due to the formation of hydroxyl groups on the surface sample. This is the first report of the use of 2,6-lutidine as a probe molecule for clarification of the formation of protonic acid sites from molecular hydrogen and the role of the tetragonal and monoclinic phases of ZrO_2.

The formation of protonic acid sites on MoO_3-ZrO_2 from molecular hydrogen was verified by a pyridine pre-adsorption IR study. Figs. 7 and 8 show the changes of the IR spectra within a range of 1600–1400 cm^{-1} when the pyridine pre-adsorbed with MoO_3-ZrO_2 was heated in hydrogen gas, followed by heating in a vacuum. Fig. 7A shows the spectral change of protonic acid sites when pyridine pre-adsorbed with MoO_3-ZrO_2 was heated from room temperature to 473 K in the presence of hydrogen gas. By increasing the temperature, the intensity of the band at 1540 cm^{-1} increased with a concomitant decrease in the intensity of the band at 1450 cm^{-1} (Fig. 7B). Although the appreciable elimination of Lewis acid sites was observed at room temperature, the formation of protonic acid sites was scarcely observed at 323 K and below. The change in protonic acid sites was significantly observed at 373 K and above. The evolution of both Lewis and protonic acid sites can be clearly seen when the absorbance bands at 1450 and 1540 cm^{-1} are plotted against the heating temperature in hydrogen (Fig. 7C). This result confirms the assistance of Lewis acid sites in the formation of protonic acid sites via a hydrogen spillover mechanism, though the pyridine probe molecule cannot be used to differentiate the role of tetragonal and monoclinic phases of ZrO_2.

The restoration of Lewis acid sites by heating in a vacuum is illustrated in Fig. 8A–C. The restoration of Lewis acid sites became appreciable at 323 K and the intensity of both Lewis and protonic acid sites was restored to original levels at 523 K. This result indicates that the formation and elimination of protonic acid sites on MoO_3-ZrO_2 caused by the contact and removal of hydrogen in gas phase is a reversible process.

The role of hydrogen gas in the *n*-alkane isomerization over MoO_3-ZrO_2 was hypothesized on the basis of catalytic isomerization of *n*-alkanes [13], in which the hydrogen in the gas phase enhanced the activity and stability of MoO_3-ZrO_2. In this study, 2,6-lutidine and pyridine IR spectroscopy were used to demonstrate the property of MoO_3-ZrO_2 in the formation of active protonic acid sites from molecular hydrogen, in which the protonic acid sites formed as active sites for *n*-heptane isomerization. The formation of active protonic acid is a reversible process; protonic acid sites are formed in the presence of hydrogen and eliminated by removal of hydrogen from the gas phase. Only Lewis acid sites corresponding to the tetragonal phase of ZrO_2 are involved in the formation of protonic acid sites. The appreciable formation began to occur at 373 K, whereas the formation of protonic acid sites from molecular hydrogen was not observed for the ZrO_2 sample (figure not shown). The absence of the specific active sites and tetragonal phase of ZrO_2 may be induced by the inability of ZrO_2 to adsorb molecular hydrogen to dissociate formed hydrogen atoms and subsequently to form protonic acid sites. The formation of protonic acid sites on MO_3-ZrO_2 may be substantiated by quantitative hydrogen adsorption on catalysts. Fig. 9 shows the variations of hydrogen uptake at 473 K as a function of time for the ZrO_2 and MO_3-ZrO_2 samples. The rate of hydrogen uptake on MoO_3-ZrO_2 was very high for the initial few minutes and the rate of adsorption then reached almost equilibrium within 3 h with a hydrogen uptake of 1.82×10^{17} H-atom/m^2-cat. In contrast, the hydrogen uptake was negligibly small for the ZrO_2 sample.

The formation of protonic acid sites from molecular hydrogen on MoO_3-ZrO_2 is basically similar to those on SO_4^{2-}-ZrO_2 and WO_3-ZrO_2 type catalysts, interpreted based on the concept of a "molecular hydrogen-originated protonic acid site" [25,40]. The protonic acid sites are generated from molecular hydrogen present in the gas phase through the dissociative adsorption of molecular hydrogen on the specific active sites followed by spillover on to

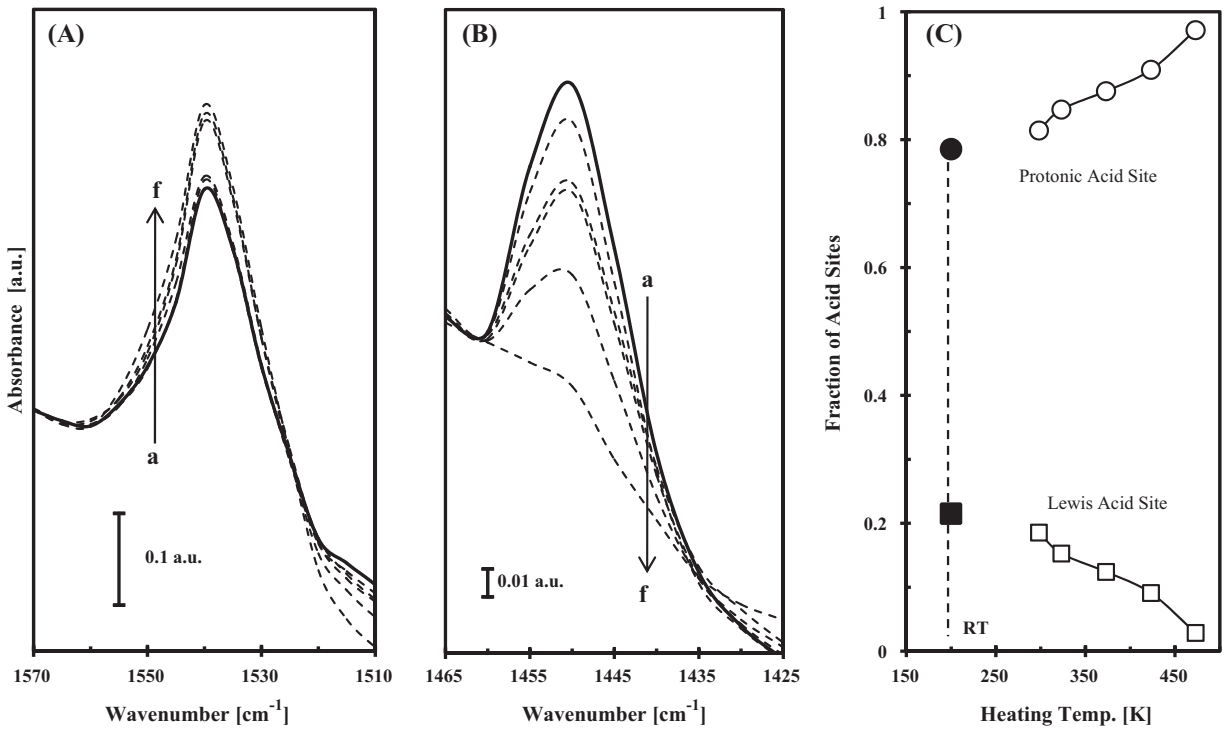

Fig. 7. IR spectra of pyridine adsorbed on MoO_3-ZrO_2. Spectral changes of (A) protonic acid sites and (B) Lewis acid sites when pyridine-preadsorbed sample was heated in hydrogen at (b) room temperature, (c) 323 K, (d) 373 K, (e) 423 K and (f) 473 K. (a) Before exposure to hydrogen. (C) The fraction of acid sites on MoO_3-ZrO_2 after heating from room temperature in the presence of hydrogen. (○) Protonic acid site; (□) Lewis acid site; (●) protonic acid sites and (■) Lewis acid sites before exposure to hydrogen at room temperature.

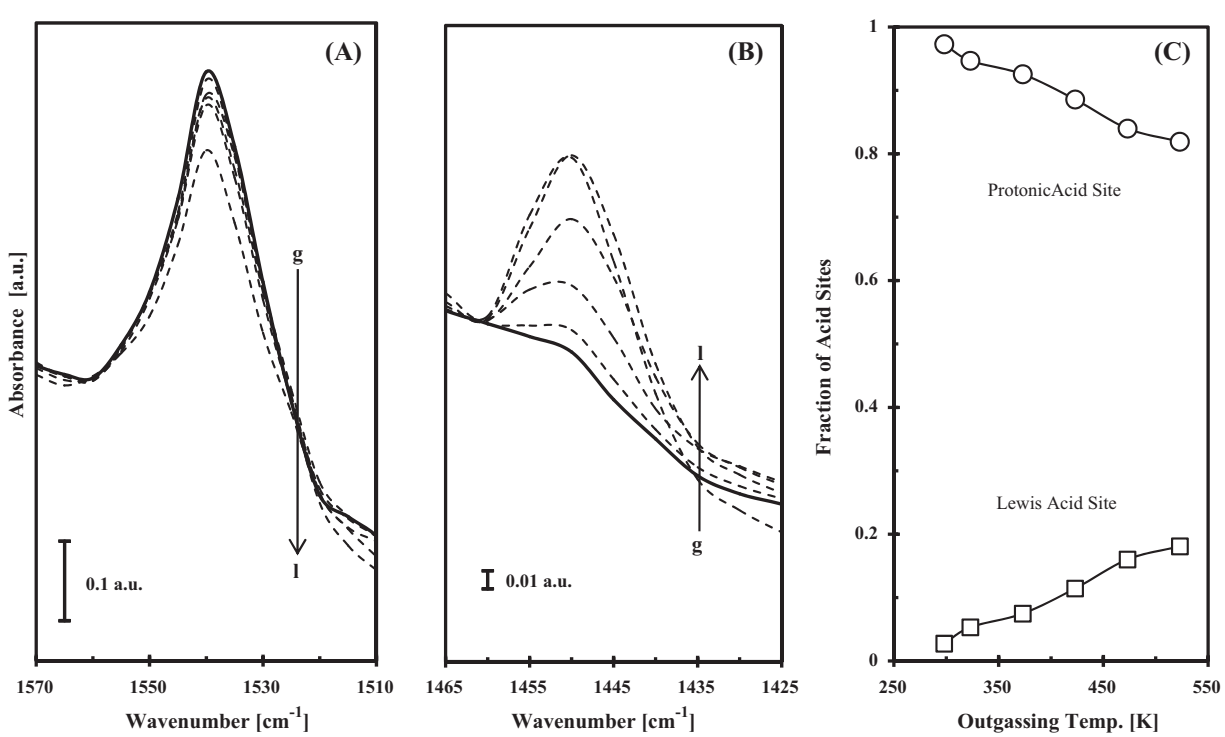

Fig. 8. Spectral changes of (A) protonic acid site and (B) Lewis acid sites when the sample of the spectrum (f) in Fig. 7 was outgassed in a vacuum at (g) room temperature, (h) 323 K, (i) 373 K, (j) 423 K, (k) 473 K and (l) 523 K. (C) The fraction of acid sites on MoO_3-ZrO_2 when heating in vacuum at different temperatures. (○) Protonic acid site and (□) Lewis acid site.

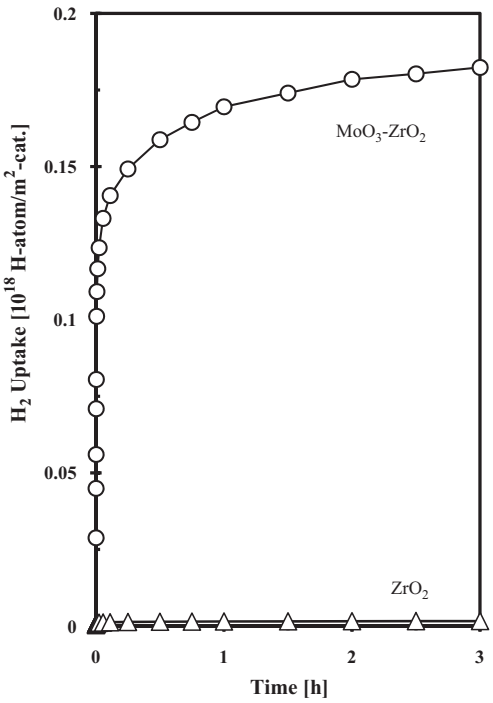

Fig. 9. Variations of hydrogen uptake on ZrO_2 and MoO_3-ZrO_2 as a function of time at 473 K. Initial hydrogen pressure was 25 Torr.

the support. The spillover hydrogen atoms diffuse over the support and reach Lewis acid sites to convert into protons and electrons in which the electrons are neutralized by Lewis acid sites. Similar to that of WO_3-ZrO_2, formation of protonic acid sites on MoO_3-ZrO_2 began to occur considerably at 373 K, though the number of protonic acid sites formed and the capacity of hydrogen uptake were different [25,41]. Both catalysts showed high activity for *n*-alkane isomerization in the absence of specific active sites such as Pt or Pd; however, WO_3-ZrO_2 is reported to be more active than that of MoO_3-ZrO_3 [42,43], which might be related to the different acid strength distribution of both samples. Although, a higher temperature is required to form protonic acid sites for SO_4^{2-}-ZrO_2 due to the slow surface diffusion of hydrogen atoms on SO_4^{2-}-ZrO_2 compared to those of WO_3-ZrO_2 and MoO_3-ZrO_2 [25,26]. In addition, specific active site such as Pt or Pd metal is indispensable for SO_4^{2-}-ZrO_2 to adsorb and dissociate molecular hydrogen, and to activate the catalyst. In contrast, although the active site types are not known for certain, WO_3-ZrO_2 and MoO_3-ZrO_2 seem to have active sites for dissociative-adsorption of molecular hydrogen to form active sites for isomerization.

3.4. Hydrogenation of 2,6-lutidine and pyridine

Fig. 10 shows the IR spectral changes for 2,6-lutidine and pyridine preadsorbed MoO_3-ZrO_2 heated in the presence of hydrogen at 573 K and below. There is no new distinct peak appeared except the changes of the peaks correspond to the partially elimination of Lewis acid sites and formation of protonic acid sites for both preadsorbed samples. These results indicated that the hydrogenation of 2,6-lutidine and pyridine adsorbed on acidic sites was not occurred on MoO_3-ZrO_2 at 573 K and below. Similar result was observed on WO_3-ZrO_2 in which the hydrogenation of pyridine was not observed at 473 K and below [25]. However, the hydrogenation of pyridine was observed on Pt loaded WO_3-ZrO_2 at 373 K and above. The difference is considered to be due to the difference in the ability for dissociation of hydrogen molecule in which the Pt enhances the dissociation of molecular hydrogen at room temperature and above. Hydrogenation of pyridine adsorbed on acidic sites was also reported on Pt/HZSM [44], and Pd/SiO_2-USY [45] catalysts

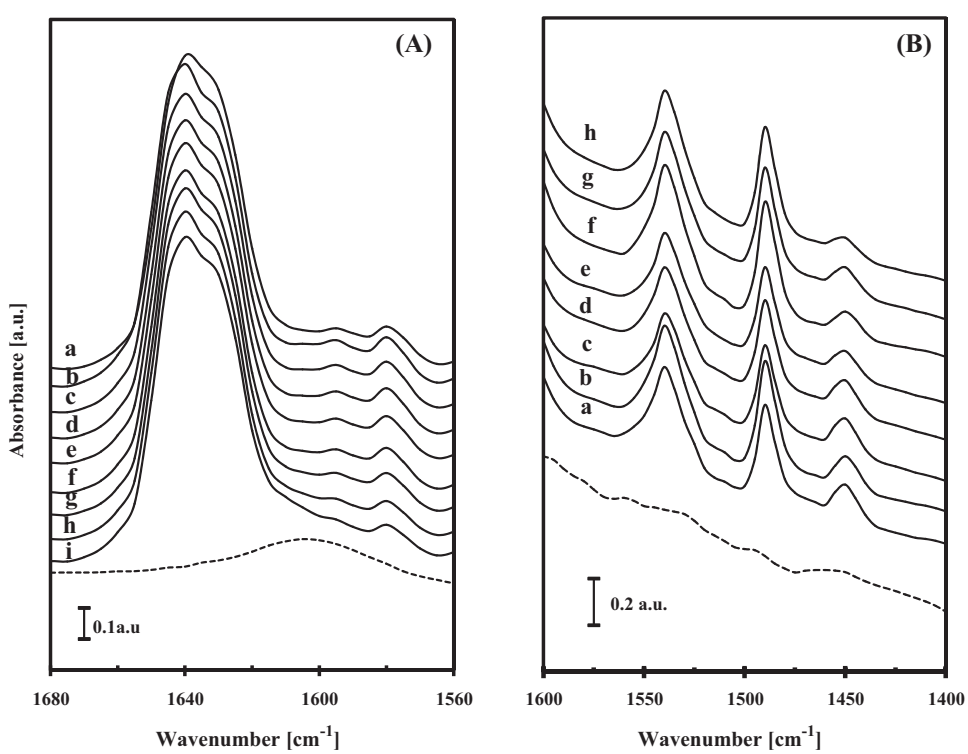

Fig. 10. (A) Spectral change for 2,6-lutidine adsorbed on MoO_3-ZrO_2 caused by heating in hydrogen at (b) 298 K, (c) 323 K, (d) 373 K, (e) 423 K, (f) 473 K, (g) 523 K, (h) 573 K, and (i) 598 K. (a) Without hydrogen. (B) Pyridine adsorbed on MoO_3-ZrO_2 followed by adsorption of hydrogen at (b) 298 K, (c) 323 K, (d) 373 K, (e) 423 K, (f) 473 K, (g) 523 K, (h) 573 K. Dotted lines represent spectra for activated MoO_3-ZrO_2.

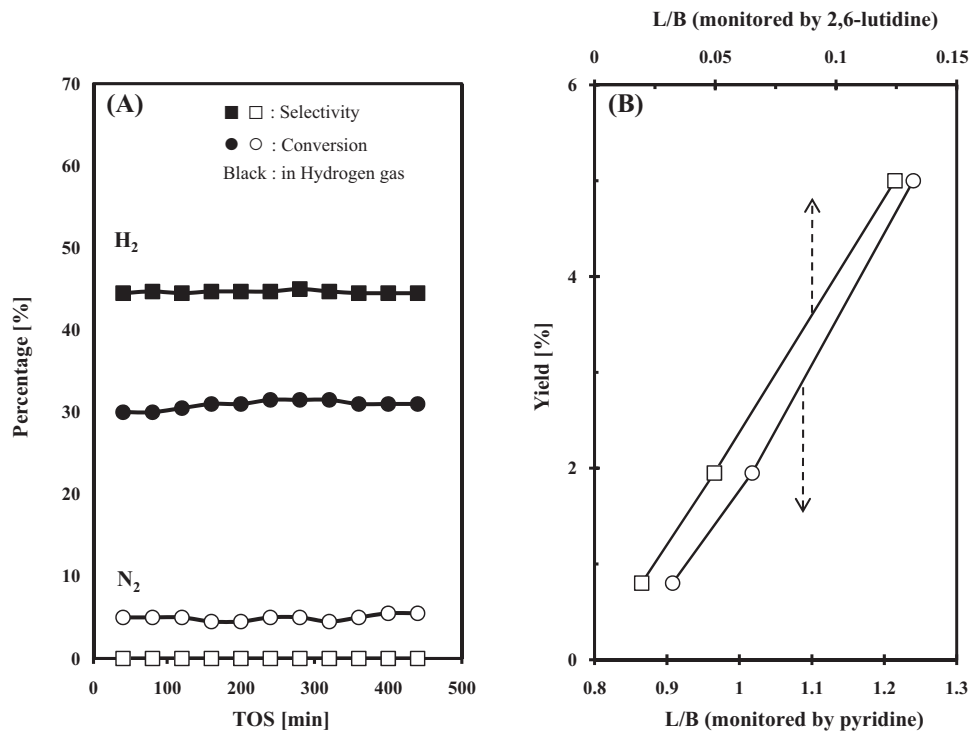

Fig. 11. (A) *n*-heptane isomerization over MoO_3-ZrO_2 at 573 K in the presence of hydrogen (black symbol) and nitrogen (white symbol). (B) Relation between ratio of Lewis to Brönsted acid sites (L/B) monitored by 2,6-lutidine and pyridine with the catalytic activity of MoO_3-ZrO_2.

in which the specific active sites such as Pt and Pd may enhance the dissociation of molecular hydrogen.

3.5. Isomerization of n-heptane

Fig. 11 and Table 1 illustrate the catalytic activity of MoO_3-ZrO_2 and product distribution for the isomerization of *n*-heptane at 573 K in an online microcatalytic reactor. For *n*-heptane isomerization at 573 K, the activity and stability of MoO_3-ZrO_2 was observed when the reaction was conducted in the presence of hydrogen in the gas phase (Fig. 11A). Only the cracking product was observed for the reaction in the presence of nitrogen. Although, the mechanism of cracking over MoO_3-ZrO_2 is not clear yet at present, it is plausible that the presence of strong acidic sites enhance the formation of cracking product in the absence of hydrogen. The relationship between the activity of MoO_3-ZrO_2 and the number of acidic sites was clearly observed in Fig. 11B. The 2,6-lutidine and pyridine IR studies proved that the ratio of Lewis to Brönsted acid sites determines catalyst activity. Particularly, an increase in the number of Lewis acid sites increased the catalytic activity of the sample due to the role of Lewis acid sites in facilitating the formation of active protonic acid sites. However, the role of Brönsted acid sites is not clear at present and most probably the existence of Brönsted acid sites in this experiment does not have much influence on the activity of the sample. In fact, although MoO_3-ZrO_2 possesses a large number of Brönsted acid sites, no isomer product was detected for *n*-heptane isomerization in the presence of nitrogen gas (Table 1).

Table 1
Distribution of products on the isomerization of *n*-heptane at 573 K in the presence of hydrogen.

	Activation temperature [K]			
	573	598	623	673
Conversion (%)	8	13	20	31(5)
Selectivity (%):				
C_1–C_2	43.5	31.7	30.1	13.3(35)
C_3–C_4	21.5	19.8	18.6	15(45)
C_5	15.4	16.5	15	14(13)
C_6	9.6	17	11.3	13(7)
iC_7	10	15	25	44.7(0)

(): in the presence of nitrogen.

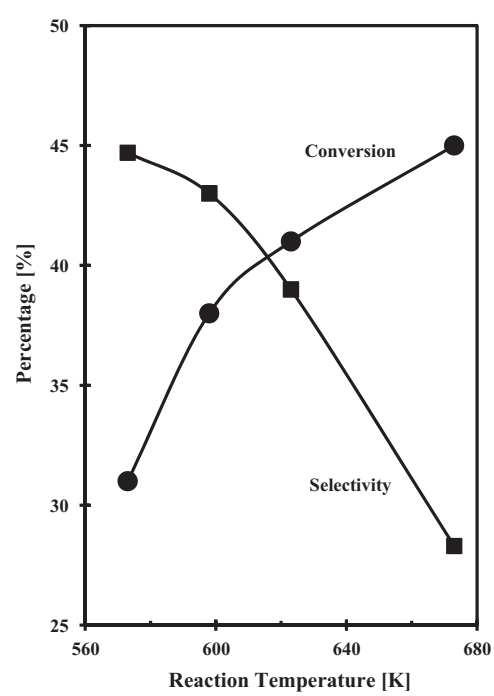

Fig. 12. Effect of reaction temperature on *n*-heptane isomerization over MoO_3-ZrO_2. Prior to the reaction, the sample was activated in hydrogen stream for 12 h at the temperature of reaction.

Hattori [40] and Barton et al. [46] also reported similar results in which strong Lewis acid sites acted as efficient catalysts for isomerization, alkylation and cracking of hydrocarbon. Importantly, ZrO_2 performed zero activity (no-isomer product) for isomerization in the presence or absence of hydrogen in this experiment (not shown), though ZrO_2 only possesses relatively strong Lewis acid sites. The effect of Lewis acid site types may be different for ZrO_2 and MoO_3-ZrO_2 due to differences in the acidic center. On the basis of the 2,6-lutidine IR study, ZrO_2 has no Lewis acid sites centered at 1595 cm^{-1} corresponding to the presence of the tetragonal phase of ZrO_2 [33]. However, the absorbance bands at 1605 and 1590 cm^{-1} on ZrO_2 and MoO_3-ZrO_2 are ascribed to the free-cus Zr^{4+} (monoclinic phase of ZrO_2). These results strongly demonstrate that the Lewis acid sites corresponding to the tetragonal phase of ZrO_2 are active sites for the formation of protonic acid sites, which is necessary in the isomerization process.

Fig. 12 shows the effect of reaction temperature on the catalytic activity of MoO_3-ZrO_2 in the presence of hydrogen. The reaction was done at temperature range of 573–673 K. Prior to the reaction, the sample was activated in hydrogen stream for 12 h at the temperature of reaction. The result indicated that increase in the reaction temperature from 573 to 673 K decrease the selectivity about 38%, while the cracking increase about 45%. The cracking increased gradually at 623 K and above. Although, the effect of acidity cannot be neglected in the reaction temperature range of 573–673 K, it is suggested that thermal cracking plays an important role in the decreasing of isomer product over this MoO_3-ZrO_2. In fact, increase the activation or reaction temperature increased slightly the number of Lewis acid sites in which the Lewis acid sites enhance the formation of active protonic acid sites. However the cracking caused by thermal effect is dominant than that of the isomerization caused by the increase in the acidity of sample.

4. Conclusions

2,6-Lutidine and pyridine pre-adsorbed IR studies indicated that MoO_3-ZrO_2 possesses a large number of relatively weak Lewis and Brönsted acid sites as well as strong Lewis and Brönsted acid sites. On the basis of the 2,6-lutidine IR study results, the formation of active protonic acid sites (bands at 1640 and 1630 cm^{-1}) from molecular hydrogen through a spillover mechanism involved the participation of strong Lewis acid sites corresponding to the tetragonal phase of ZrO_2 (bands at 1595 and 1580 cm^{-1}), while the Lewis acid sites related to the monoclinic phase of ZrO_2 disappeared in the outgassing of 2,6-lutidine at 473 K.

The activity and stability of MoO_3-ZrO_2 were observed for *n*-heptane isomerization at 573 K in which the conversion to *iso*-heptane strongly depended on the promotive effect of hydrogen as a carrier gas, whereas no activity was observed for the ZrO_2 sample due to the inability to form active protonic acid sites from molecular hydrogen. Although further, detailed study on the properties of the catalytic activity relationship is highly essential, we suggest that the role of Lewis acid sites corresponding to the tetragonal phase of ZrO_2 in the formation of active sites for isomerization is widely applicable for general acid-catalytic reactions over ZrO_2-based catalysts such as SO_4^{2-}-ZrO_2, WO_3-ZrO_2 and also Cr_2O_3-ZrO_2.

Acknowledgements

This work was supported by the Ministry of Science, Technology and Innovation, Malaysia (MOSTI) under E-Science Fund Research Projects No. 03-01-06-SF0020 and 03-01-06-SF0564. Our gratitude also goes to the Hitachi Scholarship Foundation for the Gas Chromatograph Instruments Grant.

References

[1] T. Matsuda, T. Ohno, Y. Hiramatsu, Z. Li, H. Sakagami, N. Takahashi, Appl. Catal. A 362 (2009) 40–46.
[2] V. Keller, F. Barath, G. Maire, J. Catal. 189 (2000) 269–280.
[3] F. Di-Grégorio, V. Keller, T. Di-Contanzo, J.L. Vignes, D. Michel, G. Maire, Appl. Catal. A 218 (2001) 13–24.
[4] H. Al-Kandari, F. Al-Kharafi, A. Katrib, Appl. Catal. A 361 (2009) 81–85.
[5] T. Baskar, K.R. Reddy, ChP. Kumar, M.R.V.S. Murthy, K.V.R. Chary, Appl. Catal. A 211 (2001) 189–201.
[6] M. Hino, K. Arata, J. Chem. Soc. Chem. Commun. 18 (1980) 851–852.
[7] A. Calafat, L. Avilán, J. Aldana, Appl. Catal. A 201 (2000) 215–223.
[8] A. Adamski, P. Zapala, P. Jakubus, Z. Sojka, Top. Catal. 52 (2009) 993–1000.
[9] P. Afanasiev, Mater. Chem. Phys. 47 (1997) 231–238.
[10] B. Samaranch, P.R. Piscina, G. Clet, M. Houalla, N. Homs, Chem. Mater. 18 (2006) 1581–1586.
[11] V. Indovina, Catal. Today 41 (1998) 95–109.
[12] F. Prinetto, G. Cerrato, G. Ghiotti, A. Chlorino, M.C. Champa, D. Gazzoli, V. Indovina, J. Phys. Chem. B 99 (1998) 5556–5567.
[13] J.C. Yori, C.L. Pieck, J.M. Parera, Catal. Lett. 64 (2000) 141–146.
[14] A.S.C. Brown, J.S.J. Hargreaves, S.H. Taylor, Catal. Lett. 57 (1999) 109–113.
[15] H. Miyata, Sh. Tokuda, T. Ono, T. Ohno, F. Hatayama, Chem. Soc. Faraday Trans. 86 (1990) 2291–2295.
[16] W. Shi, H.-Y. Liu, D.-M. Ren, Z. Ma, W.-D. Sun, Chem. Res. Chin. Univ. 22 (2006) 364–367.
[17] C. Kenney, Y. Maham, A.E. Nelson, Thermochim. Acta 434 (2005) 55–61.
[18] J.R. Sohn, S.G. Lee, D.C. Shin, Bull. Korean Chem. Soc. 27 (2006) 1623–1632.
[19] M. Hino, K. Arata, Mater. Chem. Phys. 26 (1990) 213–237.
[20] M. Hino, K. Arata, Appl. Catal. A 169 (1998) 151–155.
[21] S. Triwahyono, Z. Abdullah, A.A. Jalil, J. Nat. Gas Chem. 15 (2006) 247–252.
[22] J.R. Sohn, E.W. Chun, Y. Pae, Bull. Korean Chem. Soc. 24 (2003) 1785–1792.
[23] H. Toraya, S. Yoshimura, J. Am. Ceram. Soc. 67 (1984) 119–121.
[24] S. Triwahyono, T. Yamada, H. Hattori, Appl. Catal. A 250 (2003) 75–81.
[25] S. Triwahyono, T. Yamada, H. Hattori, Appl. Catal. A 242 (2003) 101–109.
[26] S. Triwahyono, A.A. Jalil, M. Musthofa, Appl. Catal. A 372 (2010) 90–93.
[27] S. Triwahyono, A.A. Jalil, H. Hattori, J. Nat. Gas Chem. 16 (2007) 252–257.
[28] S. Triwahyono, A.A. Jalil, S.N. Timmiati, N.N. Ruslan, H. Hattori, Appl. Catal. A 372 (2010) 103–107.
[29] S. Triwahyono, T. Yamada, H. Hattori, Catal. Lett. 85 (2003) 109–115.
[30] S.X. Chen, E. Iglesia, A.T. Bell, J. Catal. 189 (2000) 421–430.
[31] M. Scheithauer, R.K. Grasseli, H. Knozinger, Langmuir 14 (1998) 3019–3029.
[32] A. Corma, C. Rodelas, V. Fornes, J. Catal. 88 (1984) 374–381.
[33] C. Morterra, G. Meligrana, G. Cerrato, V. Solinas, E. Rombi, M.F. Sini, Langmuir 19 (2003) 5256–5344.
[34] B. Samaranch, P.R. Piscina, G. Clet, M. Houalla, P. Gelin, N. Homs, Chem. Mater. 19 (2007) 1445–1451.
[35] T. Onfroy, G. Clet, M. Houalla, J. Phys. Chem. B 109 (2005) 3345–3354.
[36] K.C. Pratt, J.V. Sanders, V. Cristov, J. Catal. 124 (1990) 416–432.
[37] T. Armaroli, M. Bevilacque, M. Trombetta, A.G. Alejandre, J. Ramirez, G. Busca, Appl. Catal. A 220 (2001) 181–190.
[38] T. Okuhara, Catal. Today 73 (2002) 167–176.
[39] K. Chen, S. Xie, E. Iglesia, A.T. Bell, J. Catal. 189 (2000) 421–430.
[40] H. Hattori, Stud. Surf. Sci. Catal. 138 (2001) 3–12.
[41] S. Triwahyono, T. Yamada, H. Hattori, Appl. Catal. A 250 (2003) 65–73.
[42] M. Scheithauer, T.K. Cheung, R.E. Jentoft, R.K. Grasseli, B.C. Gates, H. Knözinger, J. Catal. 180 (1998) 1–13.
[43] S. Kuba, P. Lukinskas, R.K. Grasseli, B.C. Gates, H. Knözinger, J. Catal. 216 (2003) 353–361.
[44] A. Zhang, I. Nakamura, K. Fujimoto, J. Catal. 168 (1997) 328.
[45] R. Ueda, K. Tomishige, K. Fujimoto, Catal. Lett. 57 (1999) 145.
[46] D.G. Barton, S.L. Soled, E. Iglesia, Top. Catal. 6 (1998) 87–99.